PERGAMON

International Journal of Heat and Mass Transfer 46 (2003) 963–971

International Journal of HEAT and MASS TRANSFER

www.elsevier.com/locate/ijhmt

A theoretical study on Bunsen spray flames

Jiann-Chang Lin [a], Shuhn-Shyurng Hou [b,*], Ta-Hui Lin [a]

[a] Department of Mechanical Engineering, National Cheng Kung University, Tainan 70101, Taiwan, ROC
[b] Department of Mechanical Engineering, Kun Shan University of Technology, Tainan 71003, Taiwan, ROC

Received 18 April 2002; received in revised form 7 September 2002

Abstract

The structure of Bunsen flame tip under the influence of dilute, monodisperse inert (water) or fuel (methanol) sprays is theoretically studied using large activation energy asymptotics. A completely prevaporized mode is identified, in which no liquid droplets exist downstream of the flame. Parameters for open and closed flame tips in the analysis consist of the amount of liquid loading indicating the internal heat loss for the water spray or the internal heat loss and heat gain for the rich and lean methanol-sprays, respectively, and the (negative) stretch coupled with Lewis number (Le) which strengthens the burning intensity of the $Le > 1$ flame but weakens that of the $Le < 1$ flame, respectively. For rich methane–air flames ($Le > 1$) with water sprays (or lean methanol-spray flames with $Le > 1$), closed-tip solutions are obtained. The burning intensity of the flame tip is enhanced with either decreasing liquid-water loading (or increasing liquid-fuel loading) or increasing stretch. Conversely, the negative stretch weakens the burning intensity of a lean methane–air flame ($Le < 1$) with water sprays (or a rich methanol-spray flame with $Le < 1$) and eventually leads to tip opening, i.e., flame extinction. The burning intensity is further reduced with either increasing liquid-water (or liquid-fuel) loading or increasing stretch. Moreover, the open flame tip is further widened when either the liquid-water loading (or liquid-fuel loading) or the upstream flow velocity is increased. It is noteworthy that the gradual increase of liquid-fuel loading strengthens the burning intensity of the lean methanol-spray flame ($Le > 1$) and thus leads to the transition of flame configurations from conventional Bunsen cone through planar flame to inverted flame cone (a convex flame shape with respect to the upstream reactants). The critical value of liquid-fuel loading, at which there exists a planar flame rather than a Bunsen cone flame, is increased with either increasing upstream flow velocity or decreasing equivalence ratio.

Keywords: Bunsen flame; Dilute spray; Stretch; Lewis number; Tip opening

1. Introduction

It is well-known that flame stretch is a very important factor affecting combustion phenomena. Flames can experience either positive or negative stretch depending on the nature of the flow and the flame. For instance, stretch is positive in the (divergent) stagnation-point flow and negative along the Bunsen flame. Extensive theoretical and experimental studies [1–10] have shown that effects of stretch become especially prominent in the presence of preferential diffusion, when the mixture has nonunity Lewis number. For positively stretched flames in the stagnation-point flow, increasing stretch will weaken/extinguish a $Le > 1$ flame but intensify a $Le < 1$ flame [1–4]. The converse holds for the negatively stretched Bunsen flame tip [5–10].

Sivashinsky [5,6] first analyzed the structure of the Bunsen flame tip by using activation energy asympotics. Buckmaster [7] further explored the mathematical description of open and closed Bunsen flame tips. It was generally concluded that for the negatively stretched Bunsen flame tip, since the concave shape with respect to the upstream reactants focuses the heat ahead of the flame while at the same time defocuses the reactants approaching the flame, the burning intensity is

* Corresponding author. Tel.: +886-6-272-4833; fax: +886-6-273-4240.
E-mail address: sshou@mail.ksut.edu.tw (S.-S. Hou).

0017-9310/03/$ - see front matter
PII: S0017-9310(02)00372-1

Nomenclature

Dimensional quantities

B'	preexponential factor
C'_{PG}	specific heat of the gaseous mixture
C'_{PL}	specific heat of the liquid
d'	tube diameter
E'_a	activation energy
ℓ'_D	thickness of the diffusion zone
$\widetilde{M}'$	average molar mass
$\widetilde{M}'$	molar mass
n'	number density
p'	pressure
$\widetilde{R}$	universal gas constant
r'	droplet radius
S^0_L	one-dimensional adiabatic flame speed

Nondimensional quantities

G	$d\Phi/dR$
h_{LG}	latent heat of vaporization, $h'_{LG}/(C'_{PG}T'_i)$
Le	Lewis number
$\dot{m}$	axial mass flux, ρu
Q	heat combustion of fuel, $Q'/(C'_{PG}T'_i)$
R	radial coordinate, R'/d'
T	temperature, T'/T'_i
T_a	activation temperature, $E'_a/(\widetilde{R}T'_i)$
T_f	adiabatic flame temperature, T'_f/T'_i
u	axial velocity, u'/S^0_L
W	defined in Eq. (8)
x	axial coordinate, x'/d'
Y	$Y_F = Y'_F$ and $Y_O = Y'_O/\sigma$
y	defined in Eq. (2)
z	density variable, ρ'_G/ρ'

Greek symbols

β	mass fraction perturbation in the reaction zone
γ	$(1 - z_i)/\delta$
δ	small expansion parameter, ℓ'_D/d'
ε	small expansion parameter, T_f/T_a
η	stretched variable of the reaction zone, ξ/ε
θ	temperature perturbation in the reaction zone
Λ	defined in Eq. (25)
λ'	thermal conductivity
ξ	stretched variable of the diffusion zone, y/δ
ρ'	density
σ	stoichiometric ratio
τ	defined in Eq. (29)
Φ	flame front surface
ϕ	equivalence ratio
ψ	G_0

Superscripts

$'$	dimensional quantities
$+$	downstream near the flame

Subscripts

b	boiling state
d	downstream
e	state at which droplet is completely vaporized
F, O	fuel and oxygen
f	flame front
G, L	gas and liquid phases
i	initial state
j	$j =$ F or O
k	$k =$ F and O in lean and rich mixtures, respectively
S	spray
v	state at which evaporation initiates
w	$w =$ O and F in lean and rich mixtures, respectively
0, 1	zeroth and first-orders

augmented for $Le > 1$ mixtures and diminished otherwise, which, respectively, result in the well-known interesting phenomena of tip intensification and opening (extinction). Furthermore, some experimental studies [9,10] have been reported that the observed characteristics of tip opening are essentially in agreement with the theoretical predictions [5–7]. Recently, Sung et al. [8] have analyzed the geometry, burning intensity and tip-opening of the Bunsen flame by adopting the local stretch, scalar field formulation. It was found that the tip opening for the two-dimensional flame tip is indeed possible and that the opening is widened when either Lewis number is reduced or the upstream flow velocity is increased.

Much attention has been paid to the burning and extinction of the dilute spray flame by a series of theoretical studies in one-dimensional models [11–13]. It was concluded that the flame extinction characterized by a C-shaped curve is dominated by the external heat loss, while the S-shaped extinction curve is caused by the internal heat loss associated with droplet gasification process. In those studies, however, the effects of stretch and preferential diffusion on flame behavior were not examined. Subsequently, the extinction of a positively stretched premixed flame propagating in a two-dimensional stagnation-point flow under the influence of an inert (water) spray was reported by Liu et al. [14]. Results showed that flame extinction of the $Le < 1$ flame by the inert spray is characterized by an S-shaped curve. Conversely, the $Le > 1$ flame can be extinguished with and without the participation of the inert spray.

Recently, Hou and Lin [15,16] further formulated an extinction theory of stretched premixed flames with combustible sprays in a stagnation-point flow. It was generally found that the external heat loss associated with the flow stretch dominates the trend for flame extinction and that there exists flame flashback instead of flame extinction for rich methanol-spray flames ($Le < 1$).

The previous studies on the Bunsen flame were focused on homogeneous mixtures only. Although the coupling effects of positive stretch and inert/combustible spray on premixed flames with nonunity Lewis number have been emphasized, spray effect on the negatively stretched Bunsen flame has not yet been theoretically addressed. Therefore, the aim of this work is to analyze the structure of Bunsen flame tip under the influence of an inert (water)/combustible (methanol) spray by using large activation energy asymptotics. We shall examine the flame front at distances close to the tip of Bunsen cone.

2. Configuration and assumptions

Fig. 1 shows the schematic diagram of a Bunsen flame under the influence of an inert or fuel spray. The two-phase premixture consists of gaseous fuel, air and liquid droplets. The flow velocity from the infinite distance upstream is uniform along the radial direction and is not refracted by the flame until it crosses the flame. The characteristic distance for nondimensionalization is the tube diameter d'. On the basis of large activation energy asymptotics, we simply assume that $\delta = \ell'_{\mathrm{D}}/d' \ll 1$ where $\ell'_{\mathrm{D}} = \lambda'/(\rho'_{Gi} C'_{PG} S^0_{\mathrm{L}})$ represents the thickness of diffusion zone; here λ' is the thermal conductivity, C'_{PG} is the specific heat at constant pressure, ρ'_{Gi} is the density of the fresh gas at the infinite distance upstream and S^0_{L} is the one-dimensional adiabatic laminar flame speed of a premixed flame. According to the fast chemical reaction, a thinner reaction zone is assumed to be embedded within the diffusion zone, as shown in Fig. 1.

For simplicity, we assume that the spray is monodisperse and dilute, with the amount of liquid loading being $\mathrm{O}(\varepsilon)$ of the total mixture mass. Here the small

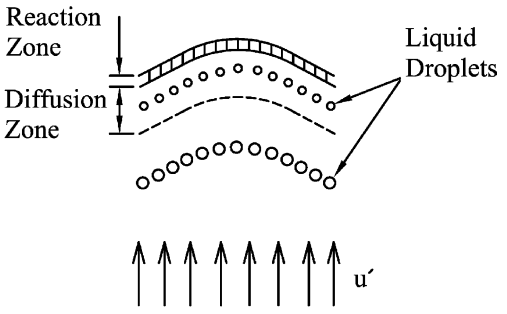

Fig. 1. The schematic diagram of a Bunsen flame under the influence of an inert/fuel spray.

parameter of expansion, $\varepsilon = T_{\mathrm{f}}/T_{\mathrm{a}} = \widetilde{R} T'_{\mathrm{f}}/E'_{\mathrm{a}}$, is the ratio of thermal energy to large activation energy in the combustion process. T_{f} denotes the adiabatic flame temperature. In the analysis, small parameters of δ and ε are assumed to be of the same order for the matching of the reaction zone. Furthermore, at the conical surfaces at the same distance parallel to the flame front, the droplets are all of the same size. The droplet temperature is constant and its motion is in phase with that of the gas. The droplets are assumed to start to evaporate only when the gas temperature has reached the boiling point of the liquid. Finally, we assume that the fuel and oxidizer reaction for the bulk premixed flame is one-step overall, that the droplet gasification follows d^2-law and that conventional constant property simplifications apply. More detailed assumptions and comments were generally described in earlier studies [11,14,16].

In the analysis, we assume that all liquid droplets are completely vaporized before reaching the flame, which is identified as a completely prevaporized model. This consideration will narrow down the applicable range of droplet size herein. However, the influence of liquid loading on the structure of Bunsen flame can be examined completely. It is apparent that the spray effect can be investigated by two parameters, namely the liquid loading and droplet size. According to our previous studies [11–16], the internal heat transfer associated with droplet vaporization can be adequately represented by investigating the completely prevaporized sprays in which no liquid droplet exists downstream of the flame. Moreover, Jones and Nolan [17] suggested that fine water spray may have a wider application in the field of combustion suppression than previously anticipated.

3. Formulation

3.1. Governing equations

From the assumptions introduced above, the total number of droplets crossing any conical surface parallel to the flame front is constant

$$n'u' = n'_i u'_i, \tag{1}$$

where n' is the number density and u' is the axial velocity. We designate the extent of gas-phase heterogeneity by the variable $z = \rho'_{\mathrm{G}}/\rho'$, where ρ' is the overall density of the two-phase mixture, and $\rho' = \rho'_{\mathrm{G}} + \rho'_{\mathrm{S}}$, in which $\rho'_{\mathrm{S}} = 4/3\pi(r'_i)^3 n' \rho'_{\mathrm{L}}$ shows the spray density. Note that $z = 1$ represents the completely vaporized state. The characteristic velocity for nondimensionalization is S^0_{L} such that $u = u'/S^0_{\mathrm{L}}$. Here, quantities with and without primes are dimensional and nondimensional, respectively. After the nondimensional governing equations in the cylindrical coordinate system (R, x) based on cylindrical symmetry were formulated, it will be convenient

to examine the problem by transforming the cylindrical coordinate system (R, x) into the (R, y) coordinate system relative to the surface of the flame front:

$$y = x - \Phi(R), \tag{2}$$

where $x = \Phi(R)$ is the equation for the surface of the flame front. Therefore, the nondimensional equations for overall continuity, gas-phase continuity, and conservation of fuel, oxidizer and energy are, respectively, given by

$$\frac{\partial}{\partial y}(\rho u) = 0, \tag{3}$$

$$\frac{\partial}{\partial y}(z\rho u) = \delta^{-1}A(1-z)^{1/3}(1-z_i)^{2/3}K(T,Y_{\mathrm{O}})/(zT), \tag{4}$$

$$\frac{\partial}{\partial y}(z\rho u Y_{\mathrm{F}}) - \delta Le_{\mathrm{F}}^{-1}\left\{\frac{\partial^2 Y_{\mathrm{F}}}{\partial y^2} + \frac{1}{R}\frac{\partial}{\partial R}\left[R\left(\frac{\partial Y_{\mathrm{F}}}{\partial R} - G\frac{\partial Y_{\mathrm{F}}}{\partial y}\right)\right] - G\frac{\partial}{\partial y}\left(\frac{\partial Y_{\mathrm{F}}}{\partial R} - G\frac{\partial Y_{\mathrm{F}}}{\partial y}\right)\right\} = \delta^{-1}W + k_{\mathrm{F}}\frac{\partial}{\partial y}(z\rho u), \tag{5}$$

$$\frac{\partial}{\partial y}(z\rho u Y_{\mathrm{O}}) - \delta Le_{\mathrm{O}}^{-1}\left\{\frac{\partial^2 Y_{\mathrm{O}}}{\partial y^2} + \frac{1}{R}\frac{\partial}{\partial R}\left[R\left(\frac{\partial Y_{\mathrm{O}}}{\partial R} - G\frac{\partial Y_{\mathrm{O}}}{\partial y}\right)\right] - G\frac{\partial}{\partial y}\left(\frac{\partial Y_{\mathrm{O}}}{\partial R} - G\frac{\partial Y_{\mathrm{O}}}{\partial y}\right)\right\} = \delta^{-1}W + k_{\mathrm{O}}\frac{\partial}{\partial y}(z\rho u), \tag{6}$$

$$\frac{\partial}{\partial y}(z\rho u T) - \delta\left\{\frac{\partial^2 T}{\partial y^2} + \frac{1}{R}\frac{\partial}{\partial R}\left[R\left(\frac{\partial T}{\partial R} - G\frac{\partial T}{\partial y}\right)\right] - G\frac{\partial}{\partial y}\left(\frac{\partial T}{\partial R} - G\frac{\partial T}{\partial y}\right)\right\} = -\delta^{-1}WQ + k_T\frac{\partial}{\partial y}(z\rho u), \tag{7}$$

where $G = \mathrm{d}\Phi/\mathrm{d}R$, $A = 3(\ell'_{\mathrm{D}})^2 p'\overline{\widetilde{M}}'/[T'_i\rho'_{\mathrm{L}}\widetilde{R}(r'_i)^2]$, and

$$W = -(B'\sigma/\widetilde{M}'_{\mathrm{O}})(p'\overline{\widetilde{M}}'/\widetilde{R})^2 \times\left\{\lambda'/[C'_{PG}(\rho'_{\mathrm{G}i}S^0_{\mathrm{L}})^2]\right\}Y_{\mathrm{O}}Y_{\mathrm{F}}\exp(-T_{\mathrm{a}}/T). \tag{8}$$

In Eqs. (4)–(7), the function $K(T, Y_{\mathrm{O}})$ and the constant parameters k_{F}, k_{O} and k_T are, respectively, $\ln[1+(T-T_{\mathrm{b}})/h_{\mathrm{LG}}]$, 1, 0 and $-h_{\mathrm{LG}}$ for the vaporizing droplet and $\ln[1+(T-T_{\mathrm{b}}+Y_{\mathrm{O}}Q)/h_{\mathrm{LG}}]$, 0, −1 and $(Q-h_{\mathrm{LG}})$ for the burning droplet.

The problem will be separately analyzed by the following two regions, namely the diffusion zone and the reaction zone. Based on the assumption of ε and δ being of the same order, the stretched variables are given by $\xi = y/\delta$ and $\eta = \xi/\varepsilon$ for the diffusion zone and the reaction zone, respectively.

3.2. The diffusion zone

In the diffusion zone, the dependent variables are expanded with respect to the same parameter of δ as

$$T = T_0 + \delta T_1 + \mathrm{O}(\delta^2), \tag{9}$$

$$Y_j = Y_{j0} + \delta Y_{j1} + \mathrm{O}(\delta^2), \quad j = \mathrm{F},\mathrm{O}, \tag{10}$$

$$u = u_0 + \delta u_1 + \mathrm{O}(\delta^2), \tag{11}$$

$$\rho = \rho_0 + \delta\rho_1 + \mathrm{O}(\delta^2), \tag{12}$$

$$G = G_0 + \delta G_1 + \mathrm{O}(\delta^2). \tag{13}$$

In order to satisfy the flame structure, z is also expanded as $z = 1 - \delta\gamma z_0 + \mathrm{O}(\delta^2)$ such that $z_i = 1 - \delta\gamma$ for a dilute spray. The liquid loading will be characterized by the parameter γ. Substituting Eqs. (9)–(13) into Eqs. (3), (5), (6) and (7) and expanding, we have

$$\frac{\partial}{\partial\xi}(\rho_0 u_0) = \frac{\partial}{\partial\xi}(\dot{m}_0) = 0, \tag{14}$$

$$\dot{m}_0\frac{\partial Y_{j0}}{\partial\xi} - \frac{1}{Le_j}(1+G_0^2)\frac{\partial^2 Y_{j0}}{\partial\xi^2} = 0, \quad j = \mathrm{F},\mathrm{O}, \tag{15}$$

$$\dot{m}_0\frac{\partial T_0}{\partial\xi} - (1+G_0^2)\frac{\partial^2 T_0}{\partial\xi^2} = 0 \tag{16}$$

from which the zeroth-order solutions are readily determined to be

$$Y_{j0} = \begin{cases} Y_{j,i} - Y_{j,i}\exp\left(\dfrac{\dot{m}_0}{1+G_0^2}Le_j\xi\right), & j = \mathrm{F},\mathrm{O}, \quad \xi < 0, \\ Y_{j,i} - Y_{k,i}, & \xi > 0, \end{cases} \tag{17}$$

$$T_0 = \begin{cases} 1 + (T_{\mathrm{f}} - 1)\exp\left(\dfrac{\dot{m}_0}{1+G_0^2}\xi\right), & \xi < 0, \\ T_{\mathrm{f}}, & \xi > 0, \end{cases} \tag{18}$$

where $k = \mathrm{F}$ and $k = \mathrm{O}$ for lean and rich mixtures, respectively. $\dot{m}_0$ is a constant and denotes the axial mass flux.

Using Eqs. (4) and (18), we find

$$z_0 = \left\{1 - \frac{2A}{3\dot{m}_0}\int_{\xi_{\mathrm{v}}}^{\xi}\left[1. + (T_{\mathrm{f}}-1)\exp\left(\frac{\dot{m}_0}{1+G_0^2}\xi\right)\right]^{-1} \times\ln\left[1 + \frac{(1-T_{\mathrm{b}}) + (T_{\mathrm{f}}-1)\exp\left(\dfrac{\dot{m}_0}{1+G_0^2}\xi\right)}{h_{\mathrm{LG}}}\right]\mathrm{d}\xi\right\}^{3/2}, \quad \xi < 0. \tag{19}$$

From Eq. (18), while the position (ξ_{v}) for the initiation of droplet evaporation is given by

$$\xi_{\mathrm{v}} = [(1+G_0^2)/\dot{m}_0]\ln[(T_{\mathrm{b}}-1)/(T_{\mathrm{f}}-1)]. \tag{20}$$

3.3. The reaction zone

In the reaction zone of the bulk gas-phase flame, the solution is expanded around the flame-sheet limit as

$$T = T_f + \varepsilon T_f \theta + O(\varepsilon^2), \tag{21}$$

$$Y_j = T_{jf} + \varepsilon \beta_j + O(\varepsilon^2), \quad j = F, O, \tag{22}$$

to result in

$$Le_j^{-1}(1+G_0^2)\frac{\partial^2 \beta_j}{\partial \eta^2} = \frac{\Lambda}{2}\left(\frac{T_f}{T_a}\right) Y_{wd}\beta_k \exp(\theta), \tag{23}$$

$$-(1+G_0^2)T_f\frac{\partial^2 \theta}{\partial \eta^2} = \frac{\Lambda}{2} Q\left(\frac{T_f}{T_a}\right) Y_{wd}\beta_k \exp(\theta), \tag{24}$$

where

$$\Lambda = 2(T_f/T_a)(B'\sigma/\widetilde{M}'_O)(p'\overline{\overline{M}}'/\widetilde{R})^2 \times \left\{\lambda'/[C'_{PG}(\rho'_{Gi}S_L^0)^2]\right\}\exp(-T_a/T_f) \tag{25}$$

is the flame speed eigenvalue and $w = O$ ($w = F$) for lean (rich) mixtures. By using the matching conditions at $\eta \to \pm\infty$, we find

$$T_1(0^+) = -2T_f \ln\left\{[(1+G_0^2)^{1/2}/\dot{m}_0] \times [T_f/(QY_{k,i})][\Lambda(T_f/T_a)Y_{wd}Le_k]^{1/2}\right\} \tag{26}$$

in which $T_1(0^+)$ denotes the first-order downstream temperature near the flame. Adding Eq. (5) or (6) to Eq. (7), and then integrating it from $\xi = -\infty$ to $\xi = 0^+$ yields

$$T_1(0^+) = \gamma\left\{T_b - \frac{C'_{PL}}{C'_{PG}}(T_b - 1) - (T_f - k_T) + \frac{\dot{m}_0}{1+G_0^2}(T_f - k_T)\int_0^{\xi_e} \exp\left(-\frac{\dot{m}_0}{1+G_0^2}\right) z_0\, d\xi\right\} - \frac{1}{\dot{m}_0}\frac{(T_f-1)(Le_k-1)}{Le_k}\left(\frac{G_0}{R} + \frac{dG_0}{dR}\right). \tag{27}$$

Combining Eqs. (26) and (27) by eliminating $T_1(0^+)$, and introducing new variables

$$\psi = G_0 \tag{28}$$

and

$$\tau = \left\{2Le_k\dot{m}_0/[(T_f-1)(Le_k-1)]\right\}R \tag{29}$$

we have

$$\frac{d\psi}{d\tau} + \frac{\psi}{\tau} = T_f \ln\left\{\frac{(1+\psi^2)^{1/2}}{\dot{m}_0}\frac{T_f}{QY_{k,i}}\left[\Lambda\left(\frac{T_f}{T_a}\right)Y_{wd}Le_k\right]^{1/2}\right\} + \frac{\gamma}{2}\left[T_b - \frac{C'_{PL}}{C'_{PG}}(T_b-1) - (T_f - k_T) + \frac{\dot{m}_0}{1+\psi^2}(T_f - k_T)\int_0^{\xi_e}\exp\left(-\frac{\dot{m}_0}{1+\psi^2}\xi\right) z_0\, d\xi\right]. \tag{30}$$

Here ψ, defined in Eq. (28), denotes the slope of the surface of the flame front and τ, defined in Eq. (29), indicates the combined effects of Lewis number and radial position. Clearly, $\tau > 0$ and $\tau < 0$, respectively, correspond to the problems of $Le > 1$ and $Le < 1$. The first term on the right hand side of Eq. (27) shows the spray effect, and the second term represents the coupling effects of Lewis number and stretch. Correspondingly, in Eq. (30) the first term and the second term on the right hand side, respectively, show the coupling effects of Lewis number and stretch, and the spray effect.

4. Results and discussion

Sample calculations are conducted by using Eqs. (26)–(30). Parameters for open and closed flame tips in the analysis consist of the amount of liquid loading (γ), and the (negative) stretch coupled with Lewis number (Le). Here γ indicates the internal heat loss for the water spray and also the internal heat transfer (heat loss or heat gain) for the fuel spray. Flame stretch is manifested through the curvature along the Bunsen flame surface, especially in the tip region, which has the largest curvature. Lewis number designates the ratio of thermal-to-mass diffusivities of the deficient reactant in the mixture. Rich and lean methane–air premixtures (or lean and rich methanol–air premixtures), respectively, corresponding to $Le > 1$ and $Le < 1$, are adopted to show the influence of nonunity Lewis number.

4.1. Methane flames without water sprays

In order to clarify the spray effects on flame behavior and clearly describe the related combustion characteristics, it is helpful to present the results of homogeneous mixture from the previous analysis [6] in the first part of discussions. It is interesting to note that by setting $\gamma = 0$ to approach the burning for homogeneous mixtures, Eq. (30) therefore degenerates to the resultant equation formulated by Sivashinsky [6]. Fig. 2 is essentially a reproduction of [6,8]. It illustrates the results of methane–air flames without water sprays. It is apparent from Eq. (29) that $\tau > 0$ and $\tau < 0$ correspond to the problems of $Le > 1$ and $Le < 1$, respectively. For $\tau < 0$ ($Le < 1$), a single integral curve (curve A) exists extending from the negative asymptotic value at $\tau = -\infty$, then decreases monotonically in approaching the symmetry axis and eventually reaches the value $\psi = -\infty$ at $\tau = 0$. Thus, as the tip is approached ($\tau = 0$), the front surface is bent out in such a way that the propagation velocity relative to the oncoming gas falls to zero. In other words a conical flame with an open-tip for $Le < 1$ is observed. Here ψ denotes the slope of the surface of the flame front. For $\tau > 0$ ($Le > 1$), a cluster of integral curves emanates from the negative asymptotic value at $\tau = +\infty$. Within this family, however, there is only one curve (curve B) corresponding to a closed-tip Bunsen

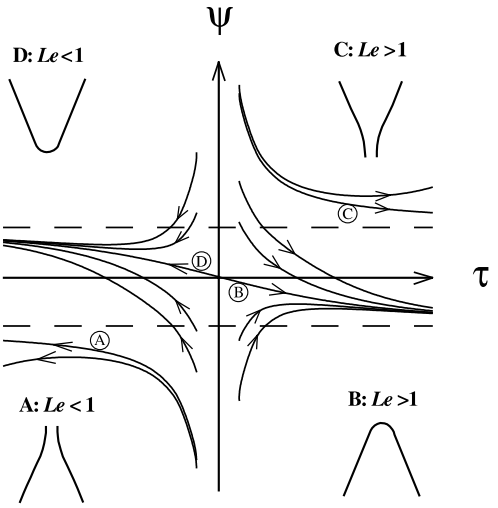

Fig. 2. The phase plane of Eq. (30) with $\gamma = 0$ [6,8]. (The arrows indicate increasing R).

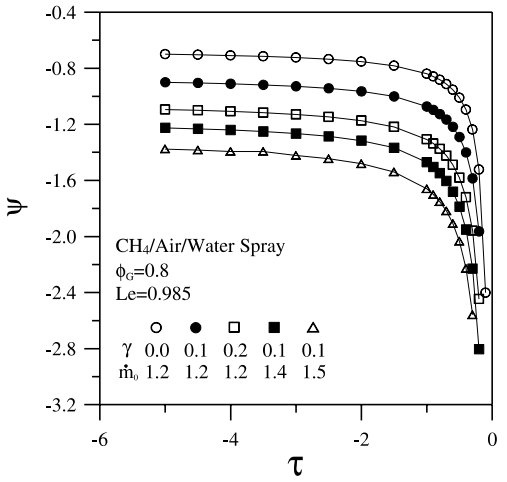

Fig. 3. The influences of liquid-water loading (γ) and axial mass flux ($\dot{m}_0$) on the structure of Bunsen flame for lean methane–air mixtures.

cone for which $\psi(0) = 0$. Furthermore, it is interesting to note that the integral curves of Eq. (30), for which ψ approaches positive asymptotic value at $\tau = \pm\infty$ may have an open-tip inverted Bunsen cone (curve C) or a continuous inverted Bunsen cone (curve D) depending on whether the mixture Lewis number is greater or less than unity, respectively, [6,8].

4.2. Methane flames with water sprays

For the lean methane–air flame ($\phi_G = 0.8$ and $Le = 0.985$), the influences of liquid loading (γ) and axial mass flux ($\dot{m}_0$) on the structure of Bunsen flame tip are depicted in Fig. 3. As just discussed, for mixtures with $Le < 1$, the negative stretch weakens the burning intensity of the flame and eventually leads to the open flame tip. For fixed γ and $\dot{m}_0$, increasing τ (increasing stretch) results in the decrease of ψ (a diminution in burning intensity) due to the augmentation of $Le < 1$ effect. As the tip is approached ($\tau = 0$), the value of ψ decreases abruptly to $-\infty$ corresponding to the phenomenon of tip opening. For a fixed $\dot{m}_0 = 1.2$, with increasing γ (increasing internal heat loss associated with water vaporization), the burning intensity is reduced such that the open flame tip is widened.

At any point in the flame front, the local flame velocity equals the component of the stream velocity normal to the flame front. At $\dot{m}_0 = 1.2$, the weakened flame with the larger γ moves downstream in order to restore dynamic equilibrium. Accordingly, the slope (ψ) of the surface of the flame front is reduced (corresponding to the reduction of the cone angle of the flame) at the same radial position (τ). Fig. 3 also shows that the $Le < 1$ flame with $\gamma = 0.1$ propagates downstream for dynamic equilibrium with increasing $\dot{m}_0$; and thus ψ decreases at the same radial position. Furthermore, the open flame tip is widened with increasing $\dot{m}_0$ due to increased upstream flow velocity.

Fig. 4 demonstrates the influences of γ and $\dot{m}_0$ on the structure of Bunsen flame tip for rich methane–air flames ($\phi_G = 1.4$ and $Le = 1.033$). Contrary to the open flame tip for $Le < 1$ indicated in Fig. 3, for mixtures with $Le > 1$, a closed-tip Bunsen cone is expected to be indeed possible. For a fixed γ and a given $\dot{m}_0$, since stretch is manifested through the curvature along the Bunsen flame surface, ψ increases towards the flame tip for which $\psi(0) = 0$ attaining its maximum at the tip. The gradual decrease of τ leads to a monotonic increase of ψ

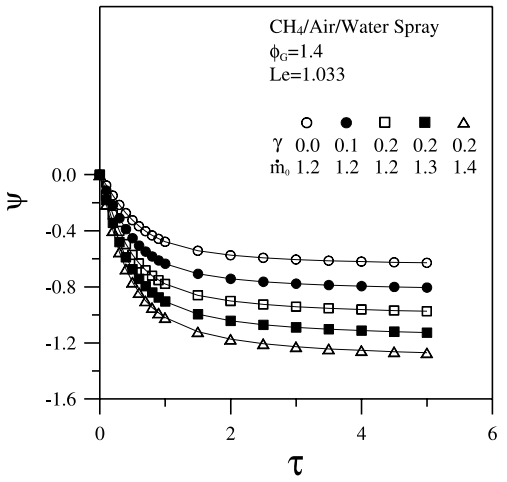

Fig. 4. The influences of liquid-water loading (γ) and axial mass flux ($\dot{m}_0$) on the structure of Bunsen flame for rich methane–air mixtures.

and thus results in tip intensification. On the other hand, the internal heat loss associated with liquid-water vaporization weakens the burning intensity of the flame because of the diminution of the total mixture enthalpy. Therefore, at $\dot{m}_0 = 1.2$, the increase of γ leads to the enlargement of internal heat loss. In order to restore dynamic equilibrium, thereby, the weakened flame with a larger γ moves downstream resulting in the decrease of ψ (the reduction of the cone angle of the flame). At $\gamma = 0.2$, increasing $\dot{m}_0$ (from 1.2 through 1.3 to 1.4) makes the flame move downstream, indicating the decrease of ψ. This phenomenon is similar to that shown in Fig. 3. Moreover, the burning intensity of $Le > 1$ flame is intensified with either increasing stretch (corresponding to decreasing τ) or decreasing γ.

4.3. Lean methanol spray flames with $Le > 1$

The influences of γ and $\dot{m}_0$ on the structure of Bunsen flame for lean methanol–air mixtures ($\phi_G = 0.8$ and $Le = 1.050$) are shown in Fig. 5. As aforementioned, for $Le > 1$ mixtures, a closed-tip Bunsen flame is observed. For the droplet gasification process in a lean spray, the liquid-fuel absorbs heat for upstream prevaporization, produces the secondary gasified fuel for bulk gas-phase burning, results in the so-called internal heat gain and thereby enhances the burning intensity of the spray flame. At $\dot{m}_0 = 1.2$, with increasing liquid-fuel loading (γ), the burning intensity of the lean methanol–air flame is strengthened owing to the increase of internal heat gain. Therefore, the flame propagates upstream leading to the increase of ψ at the same radial position. When γ is increased to a critical value ($\gamma^* = 0.057$), the flame moves further upstream and becomes a planar flame

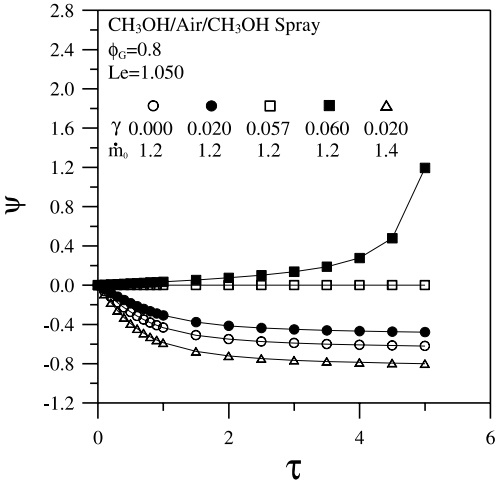

Fig. 5. The influences of liquid-methanol loading (γ) and axial mass flux ($\dot{m}_0$) on the structure of Bunsen flame for lean methanol–air mixtures.

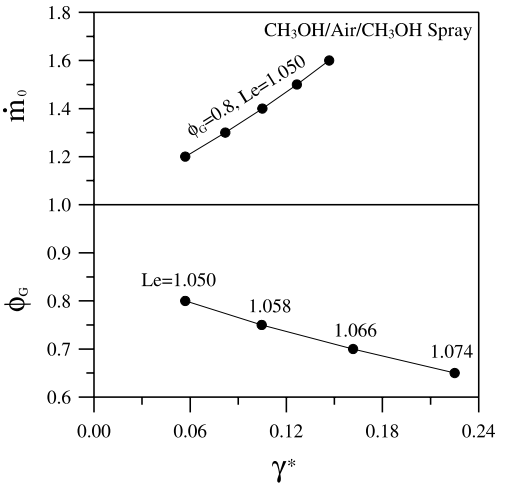

Fig. 6. The critical value γ^* as functions of the axial mass flux ($\dot{m}_0$) and the equivalence ratio (ϕ_G).

(corresponding to $\psi = 0$) rather than a Bunsen cone flame. Furthermore, as $\gamma > \gamma^* = 0.057$, e.g., $\gamma = 0.060$, inverted flame cone (a convex flame shape with respect to the upstream reactants) occurs because the value of ψ is positive. Notably, the gradual increase of γ leads to the transition of ψ from negative through zero to positive corresponding to the transition of flame configurations from conventional Bunsen flame through planar flame to inverted flame. The parameter γ^* is defined as the critical value of γ at which $\psi = 0$, denoting a planar flame.

The critical value γ^* as functions of $\dot{m}_0$ and ϕ_G is displayed in Fig. 6. For a fixed equivalence ratio ($\phi_G = 0.8$), with increasing $\dot{m}_0$ (increasing upstream flow velocity), the flame speed required for the occurrence of planar flame is enlarged. A lean methanol-spray containing a larger γ has a strengthened burning intensity due to the additional internal heat gain resulted from burning the secondary gasified fuel. Therefore, the γ^* value is increased with increasing $\dot{m}_0$, as shown in the upper half of Fig. 6. The decrease of ϕ_G, corresponding to the reduction of the burning intensity of the lean methanol flame, results in the decrease of cone angle (the decrease of ψ). Hence, for a constant $\dot{m}_0 = 1.2$, the γ^* value increases with reducing ϕ_G, as represented in the lower half of Fig. 6.

4.4. Rich methanol spray flames with $Le < 1$

Fig. 7 shows the influences of γ and $\dot{m}_0$ on the structure of Bunsen flame for rich methanol–air mixtures ($\phi_G = 1.4$ and $Le = 0.971$). For mixtures with $Le < 1$, an open-tip Bunsen cone is observed. Contrary to the lean methanol-spray, in a rich methanol-spray the liquid-fuel absorbs heat for upstream prevaporization,

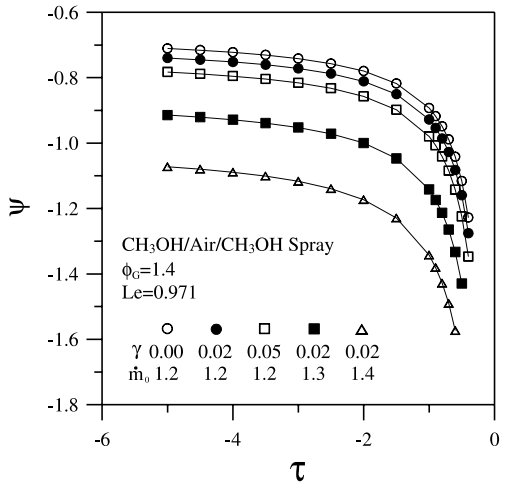

Fig. 7. The influences of liquid-methanol loading (γ) and axial mass flux ($\dot{m}_0$) on the structure of Bunsen flame for rich methanol–air mixtures.

producing the secondary gasified fuel which is equivalent to an inert substance with no contribution to burning, thus providing an overall internal heat loss, and subsequently weakening the burning intensity of the flame. Therefore, for a fixed $\dot{m}_0 = 1.2$, the $Le < 1$ flame is pushed further downstream and has a decreased ψ (corresponding to a diminished cone angle) when liquid-methanol loading (γ) is increased. For a fixed $\gamma = 0.02$, as $\dot{m}_0$ increases, the $Le < 1$ flame propagates downstream in order to restore the dynamic equilibrium, and hence ψ decreases. Note that increasing either liquid-methanol loading or stretch can further reduce the burning intensity. Furthermore, the open flame tip is widened with increasing γ or $\dot{m}_0$. These phenomena are similar to those described in Fig. 3.

5. Conclusions

A theory of negatively stretched premixed flames with inert/combustible sprays was developed using activation energy asymptotics to explore the influences of liquid spray, flame stretch, and Lewis number on the structure of Bunsen flame tip. Results are generally concluded as follows:

1. For rich methane–air flames ($Le > 1$) with water sprays, closed-tip solutions are obtained. The burning intensity of the flame tip is enhanced with either decreasing liquid loading or increasing stretch.
2. On the other hand, the negative stretch weakens the burning intensity of a lean methane–air flame ($Le < 1$) with water sprays and eventually leads to tip opening, i.e., flame extinction. The burning intensity is further reduced with either increasing liquid loading or increasing stretch. Note that the open flame tip is further widened with increasing either liquid loading or upstream flow velocity.
3. Considering the lean methanol-spray flame with $Le > 1$, the burning intensity enhanced by the negative stretch can be further increased when the spray has a larger amount of liquid-fuel loading. However, it is noteworthy that the gradual increase in liquid-fuel loading leads to the transition of flame configurations from conventional Bunsen cone through planar flame to inverted flame cone. The critical value of liquid-fuel loading, at which there exists a planar flame rather than a Bunsen cone flame, is increased with either increasing upstream flow velocity or reducing equivalence ratio.
4. Contrary to the lean methanol-spray with $Le > 1$, the secondary gasified fuel for the rich methanol-spray with $Le < 1$ is equivalent to an inert substance with no contribution to burning, thus providing an overall internal heat loss, and subsequently weakening the burning intensity of the flame. Therefore, the burning intensity is further reduced when either liquid-fuel loading or stretch is increased. Moreover, the open flame tip is widened with increasing liquid-fuel loading or upstream flow velocity. These phenomena are similar to those of the lean methane–air flame ($Le < 1$) with water sprays.

Acknowledgements

The authors would like to thank the National Science Council, Taiwan, ROC, for financially supporting this research under Contract of NSC91-2212-E-168-014. Valuable comments by the reviewers of this report are kindly appreciated.

References

[1] Y.D. Kim, M. Matalon, Propagation and extinction of a flame in a stagnation-point flow, Combust. Flame 73 (1988) 303–313.
[2] S. Ishizuka, C.K. Law, An experimental study on extinction and stability of stretched premixed flames, in: Proceedings of the Nineteenth Symposium (International) on Combustion, The Combustion Institute, 1982, pp. 327–335.
[3] J. Sato, Effects of Lewis number on extinction behavior of premixed flames in a stagnation flow, in: Proceedings of the Nineteenth Symposium (International) on Combustion, The Combustion Institute, 1982, pp. 1541–1548.
[4] H. Tsuji, I. Yamaoka, Structure and extinction of near-limit flames in a stagnation flow, in: Proceedings of the Nineteenth Symposium (International) on Combustion, The Combustion Institute, 1982, pp. 1533–1540.

[5] G.I. Sivashinsky, The diffusion stratification effect in Bunsen flames, J. Heat Transfer 96 (1974) 530–535.
[6] G.I. Sivashinsky, Structure of Bunsen flames, J. Chem. Phys. 62 (2) (1975) 638–643.
[7] J. Buckmaster, A mathematical description of open and closed flame tip, Combust. Sci. Technol. 20 (1979) 33–40.
[8] C.J. Sung, K.M. Yu, C.K. Law, On the geometry and burning intensity of Bunsen flames, Combust. Sci. Technol. 100 (1994) 245–270.
[9] C.K. Law, S. Ishizuka, P. Cho, On the opening of premixed Bunsen flame tips, Combust. Sci. Technol. 28 (1982) 89–96.
[10] M. Mizomoto, Y. Asaka, S. Ikai, C.K. Law, Effects of preferential diffusion on the burning intensity of curved flames, in: Proceedings of the Twentieth Symposium (International) on Combustion, The Combustion Institute, 1984, pp. 1933–1939.
[11] C.C. Liu, T.H. Lin, The interaction between external and internal heat losses on the flame extinction of dilute sprays, Combust. Flame 85 (1991) 468–478.
[12] S.S. Hou, C.C. Liu, T.H. Lin, The influence of external heat transfer on flame extinction of dilute sprays, Int. J. Heat Mass Transfer 36 (7) (1993) 1867–1874.
[13] S.S. Hou, T.H. Lin, A theory on excess-enthalpy spray flame, Atomization Sprays 9 (1999) 355–369.
[14] C.C. Liu, T.H. Lin, J.H. Tien, Extinction theory of stretched premixed flames by inert sprays, Combust. Sci. Technol. 91 (1993) 309–327.
[15] S.S. Hou, T.H. Lin, Extinction of stretched spray flames with nonunity Lewis numbers in a stagnation-point flow, in: Proceedings of the Twenty-Seventh Symposium (International) on Combustion, The Combustion Institute, 1998, pp. 2009–2015.
[16] S.S. Hou, T.H. Lin, Effects of internal heat transfer and preferential diffusion on stretched spray flames, Int. J. Heat Mass Transfer 44 (2001) 4391–4400.
[17] A. Jones, P.F. Nolan, Discussions on the use of fine water sprays or mist for the suppression, J. Loss Prevention Process Industries 8 (1) (1995) 17–22.